We are IntechOpen, the world's leading publisher of Open Access books Built by scientists, for scientists

6,900
Open access books available

186,000
International authors and editors

200M
Downloads

154
Countries delivered to

Our authors are among the

TOP 1%
most cited scientists

12.2%
Contributors from top 500 universities

CLARIVATE ANALYTICS
BOOK CITATION INDEX
INDEXED

WEB OF SCIENCE™

Selection of our books indexed in the Book Citation Index
in Web of Science™ Core Collection (BKCI)

Interested in publishing with us?
Contact book.department@intechopen.com

Numbers displayed above are based on latest data collected.
For more information visit www.intechopen.com

How to Expand the Workspace of Parallel Robots

Takashi Harada

Additional information is available at the end of the chapter

Abstract

In this chapter, methods for expanding the workspace of parallel robots are introduced. Firstly, methods for expanding the translational workspace of the parallel robot are discussed. The parallel robot has multiple solutions of the inverse and forward displacement analysis. By changing its configurations from one solution to another, the parallel robot can expand its translational workspace. However, conventional nonredundant parallel robot encounters singularity during the mode change. Singularity-free mode changes of the parallel robot by redundant actuation are introduced. Next, methods for expanding the rotational workspace of the parallel robot are shown. In order to achieve the large rotation, some mechanical gimmicks by gears, pulleys, and helical joints have been embedded in the moving part. A novel differential screw-nut mechanism for expanding the rotational workspace of the parallel robot is introduced.

Keywords: parallel robot, workspace, mode change, kinematics, singularity, differential, helical joint

1. Introduction

The parallel robot has excellent characteristics such as high speed, high precision, and high rigidity [1]. However, mechanical collisions between limbs and complexly existing singular configurations restrict its workspace. In this chapter, firstly, methods for expanding the translational workspace of the parallel robot are discussed. The parallel robot has multiple solutions of the inverse and forward displacement analysis. By changing its configurations from one solution to another, the parallel robot can expand its translational workspace. However, conventional nonredundant parallel robot encounters singularity during the mode change. Singularity-free mode changes of the parallel robot by redundant actuation are introduced. Next, methods for expanding the rotational workspace of the parallel robot are shown. In

order to achieve the large rotation, some mechanical gimmicks by gears, pulleys, and helical joints have been embedded in the moving part. A novel differential screw-nut mechanism for expanding the rotational workspace of the parallel robot is introduced.

2. Expanding the translational workspace

2.1. Mode change of the parallel robot

Schematic model of a planar two-dof (degree-of-freedom) serial robot and a planar two-dof parallel robot is illustrated in **Figures 1** and **2**, respectively. R and P represent the rotational pair and prismatic (sliding) pair, respectively. Underline indicates that an actuator is located at the pair, namely, $\underline{R}$ and $\underline{P}$ represent active rotational pair and active prismatic pair, and R and P represent passive ones. The serial robot in **Figure 1** is represented as $\underline{RR}$ mechanism, and the parallel robot in **Figure 2** is represented as 2$\underline{P}RR$ mechanism. In 2$\underline{P}RR$, "2" means that the two $\underline{P}RR$ mechanisms are connected to the output link (end effector or hand) in parallel. In order to control the position of the hand, forward displacement analysis gives the position and orientation of the hand from the displacements of the active pairs (joints), and inverse displacement analysis gives the displacements of the active joints from the position and orientation of the hand. As shown in **Figures 1** and **2(a)**, different solutions for inverse displacement analysis and different position of the joints for a position and orientation of the hand exist. In the robotics, the solution of the inverse displacement analysis is called as the working mode. Changing the positions of the joints between the different working modes, at that time the robot changes its configuration, is named as the working mode change. In the case of the serial robot, there exists only one solution for the forward displacement analysis; namely, when the displacement of the active joints is given, the position and orientation of the robot are fixed. However, in the case of the parallel robot, there exist different solutions for the forward displacement analysis as shown in **Figure 2(b)**. The solution of the forward displacement analysis is named as the assembly mode. Parallel robot can change the position and orientation of the hand with the same displacements of the actuated joints. Note here that the parallel robot in **Figure 2** is designed as free of the mechanical interferences such as limb collisions. Parallel robot can expand the workspace of the hand by the assembly mode change as shown in **Figure 2(b)**.
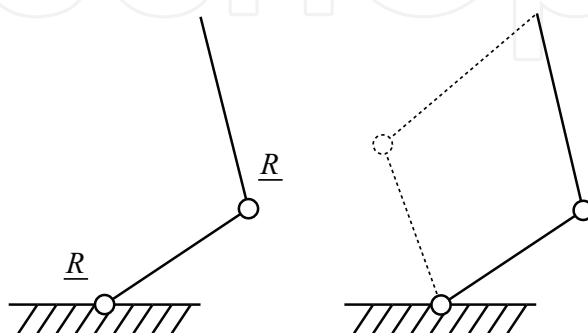

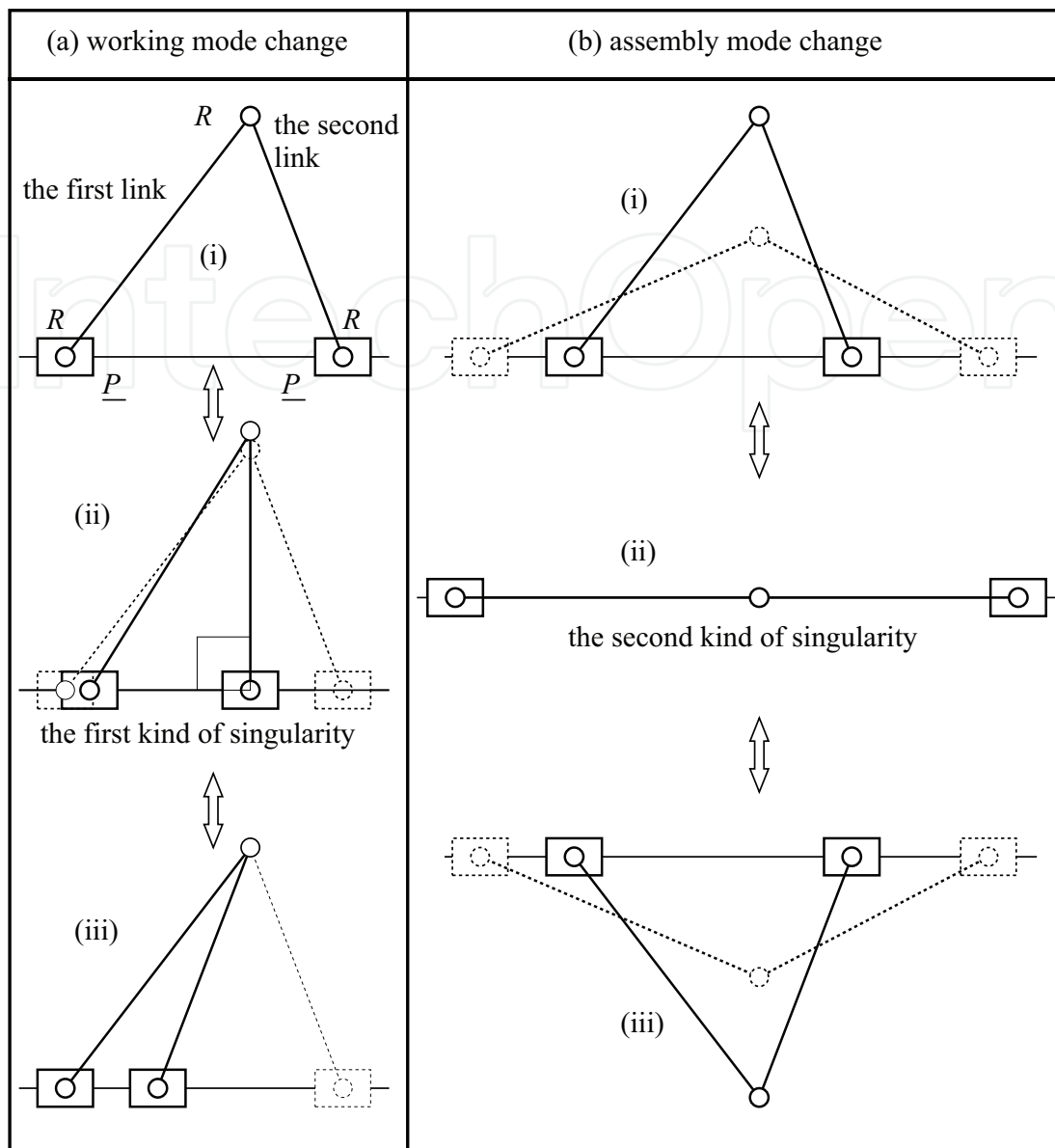**Figure 1.** Working mode change of $\underline{RR}$ serial robot.

Figure 2. Assembly and working mode change of 2*PRR* parallel robot.

2.2. Kinematics of the parallel robot

As mentioned before, the parallel robot can expand its workspace by the mode change. However, parallel robot encounters the singular configuration between the mode changes. In this section, kinematics and singular configuration of a 2*PRR* parallel robot are shown in **Figure 3**. Coordinate frames Σ_0 and Σ_i ($i = 1, 2$) are defined for the fixed coordinate and position of each actuator, respectively. Vector bi is defined for the position of the origin Σ_i with respect to the coordinate Σ_0. In the case of the 2*PRR* parallel robot in **Figure 3**, $\mathbf{b}_i = \mathbf{0}$ ($i = 1, 2$) because each coordinate Σ_i is coincident with Σ_0. Unit direction vector and displacement of the linear actuator are defined as $\mathbf{u}_i$ and $\mathbf{q}_i$, respectively. Unit direction vector and length of the rod are defined as $\mathbf{w}_i$ and l_i, respectively. Position of the hand (output link) is given as

$$\mathbf{x} = \mathbf{b}_i + q_i \mathbf{u}_i + l_i \mathbf{w}_i \tag{1}$$

Equation (1) is the loop closure equation of the parallel robot. Next, the forward displacement analysis and inverse displacement analysis of the parallel robot are going to be derived.

Eq. (1) is deformed as

$$l_i \mathbf{w}_i = \mathbf{x} - \mathbf{b}_i - q_i \mathbf{u}_i \tag{2}$$

The unit direction vector $\mathbf{w}_i$ is eliminated by raising the both sides of Eq. (2) to the second power as,

$$l_i^2 = (\mathbf{x} - \mathbf{b}_i - q_i \mathbf{u}_i)^T (\mathbf{x} - \mathbf{b}_i - q_i \mathbf{u}_i) \tag{3}$$

As shown in **Figure 3**, $\mathbf{u}_i$ and $\mathbf{b}_i$ are given as,

$$\mathbf{u}_i = \begin{bmatrix} 1 \\ 0 \end{bmatrix}, \mathbf{b}_i = \begin{bmatrix} 0 \\ 0 \end{bmatrix} \; (i = 1, 2) \tag{4}$$

Substituting Eq. (4) into Eq. (3), one obtains a quadratic equation about the displacement of the actuator as,

$$q_i^2 - 2q_i x + (y^2 - x^2 - l_i^2) = 0 \tag{5}$$

Solutions of the inverse displacement analysis are given by the solution of Eq. (5) as,

$$q_i = x \pm \sqrt{l_i^2 - y^2} \tag{6}$$

Eq. (6) represents that there are two solutions for the inverse displacement analysis. It means that the parallel robot has two working modes. **Figure 2(a)** (i) and (iii) represents the configurations of the parallel robot of the two working modes.

In the forward displacement analysis, positions x and y of the hand are solved by the simultaneous equations about Eq. (1) of each arm as,

$$\begin{cases} (x - q_1)^2 + y^2 = l_1^2 \\ (x - q_2)^2 + y^2 = l_2^2 \end{cases} \tag{7}$$

Each equation of (7) represents that a circle of the central position is $(q_i, 0)$ and the radius is l_i. The solution of Eq. (7) is given as the crossing point of the two circles. There exist two crossing points of the circles; namely, the parallel robot has two assembly modes. **Figure 2(b)** (i) and (iii) represents each configuration of the assembly mode of the parallel robot.

When $y = l_i$, at that time, the value in the square root in Eq. (6) becomes zero and the inverse displacement analysis has a duplication solution. When $y > l_i$, at that time, value in the square root in Eq. (6) becomes negative and the inverse displacement analysis has no solution. When
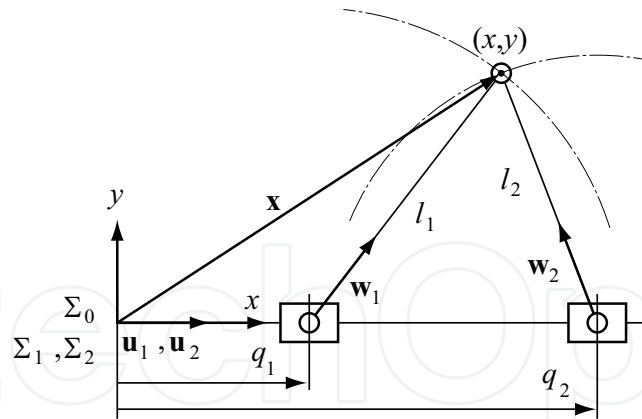
Figure 3. Kinematic model of 2*PRR* parallel robot.

the distance between the two circles of Eq. (7) equals $(l_i + l_2)$, the forward displacement analysis has a duplication solution. When the distance between the two circles of Eq. (7) becomes larger than $(l_i + l_2)$, the forward displacement analysis has no solution.

2.3. Singularity analysis of the parallel robot

2.3.1. The Jacobian of the parallel robot

Differentiating the both sides of Eq. (1) with respect to time, one obtains

$$\dot{\mathbf{x}} = \dot{q}_i \mathbf{u}_i + l_i \dot{\mathbf{w}}_i \tag{8}$$

In Eq. (1), $\mathbf{b}_i$, $\mathbf{u}_i$, and l_i are constant values and their time derivatives become zero. Because $\mathbf{w}_i$ is unit direction vector, one obtains

$$\mathbf{w}_i^T \mathbf{w}_i = 1 \tag{9}$$

Differentiating the both sides of Eq. (9) with respect to time, one obtains

$$\mathbf{w}_i^T \dot{\mathbf{w}}_i = 1 \tag{10}$$

Multiplying the both sides of Eq. (8) by $\mathbf{w}_i^T$ and taking into consideration about Eq. (9), one obtains

$$\mathbf{w}_i^T \dot{\mathbf{x}} = \mathbf{w}_i^T \mathbf{u}_i \dot{q}_i \tag{11}$$

The displacements of all actuators q_1 and q_2 are defined by vector form as $\mathbf{q} = [q_1 \ q_2]^T$; then, Eq. (10) is expressed by matrix form as

$$\mathbf{J}_x \dot{x} = \mathbf{J}_q \dot{q} \tag{12}$$

$$\mathbf{x} = \begin{bmatrix} \dot{x} & \dot{y} \end{bmatrix}^T, \mathbf{q} = \begin{bmatrix} \dot{q}_1 & \dot{q}_2 \end{bmatrix}^T$$

$$\mathbf{J}_x = \begin{bmatrix} \boldsymbol{w}_1^T \\ \boldsymbol{w}_2^T \end{bmatrix}, \mathbf{J}_q = \begin{bmatrix} \boldsymbol{w}_1^T \boldsymbol{u}_1 & 0 \\ 0 & \boldsymbol{w}_2^T \boldsymbol{u}_2 \end{bmatrix}$$

$\mathbf{J}_x$ and $\mathbf{J}_q$ are the Jacobian of the parallel robot.

2.3.2. Second kind of singularity

When the Jacobian matrix $\mathbf{J}_x$ becomes singular, namely the determinant of the Jacobian becomes zero as

$$\det(J_x) = 0 \tag{13}$$

Then, the parallel robot is in the second kind of singularity [2] or in direct kinematics singularity [3]. The 2*PRR* parallel robot occurs in the second kind of singularity when the direction of the two rods $\mathbf{w}_1$ and $\mathbf{w}_2$ becomes identical.

$$\det\left(\begin{bmatrix} \boldsymbol{w}_1^T \\ \boldsymbol{w}_2^T \end{bmatrix} \right) = 0 \tag{14}$$

This case corresponds to that two rods of the parallel robot lay in one line as shown in **Figure 2(b)** (ii). As shown in **Figure 2(b)**, the parallel robot encounters the second kind of singularity during the assembly mode change.

2.3.3. First kind of singularity

When the Jacobian matrix $\mathbf{J}_q$ is singular

$$\det(J_q) = 0 \tag{15}$$

Then, the parallel robot is in the first kind of singularity [2] or in inverse kinematics singularity [3]. The 2*PRR* parallel robot occurs in the first kind of singularity when the direction of at least one rod is perpendicular to the direction of the actuator as shown in **Figure 2(a)** (ii).

$$\det\left(\begin{bmatrix} \boldsymbol{w}_1^T \boldsymbol{u}_1 & 0 \\ 0 & \boldsymbol{w}_2^T \boldsymbol{u}_2 \end{bmatrix} \right) = 0 \tag{16}$$

As shown if **Figure 2(a)**, the parallel robot encounters the first kind of singularity during the working mode change.

2.3.4. The third kind of singularity

The third kind of singularity [2] occurs when both $\mathbf{J}_q$ and $\mathbf{J}_x$ are simultaneously singular. It requires certain conditions of the linkage parameter. In the case of the 2*PRR* parallel robot, when the lengths of the rods are identical, the third kind of singularity occurs as shown in **Figure 4**. The third kind of singularity is referred as the combined singularity [3].
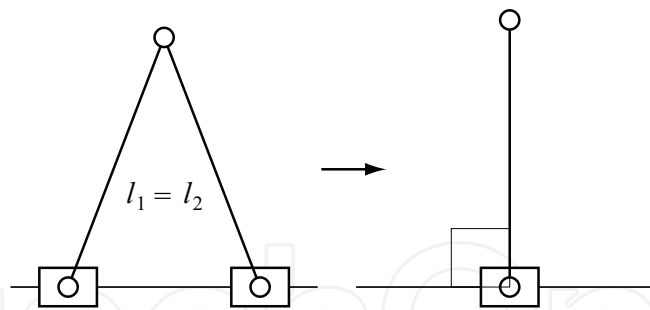
Figure 4. The third kind of singularity of the 2$\underline{P}$RR parallel robot.

2.4. Passing the singular configuration during the mode changes

2.4.1. Passing the second kind of singularity during the assembly mode change

2.4.1.1. Using the inertia

As shown in **Figure 5(a)**, if the parallel robot has some speed just before the singular configuration, the robot keeps moving according to the law of inertia; then, the parallel robot passes
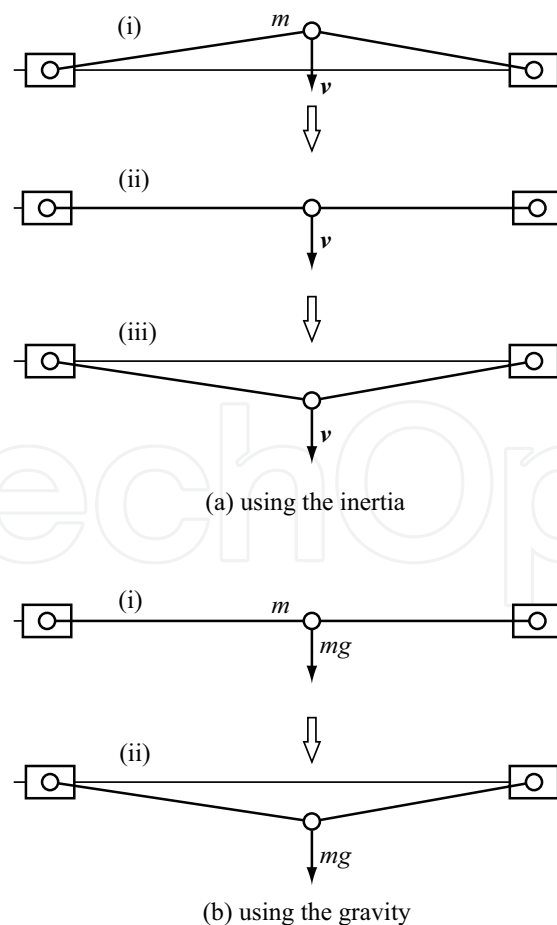

Figure 5. Assembly mode change of nonredundant 2$\underline{P}$RR parallel robot.

the second kind of singularity. Note here if the parallel robot stops at the singular configuration, it is impossible to pass the singular configuration by the inertia.

2.4.1.2. Using the gravity

As shown in **Figure 5(b)**, when the gravity force acts to the lower direction, the parallel robot can pass the singular configuration even if the parallel robot stops at the singular configuration. However, the robot cannot move to the upper direction against the gravity. When the robot moves on the horizontal plane where the gravity force does not act on the robot, the parallel robot cannot pass the singular configuration.

2.4.1.3. Using the redundancy

A robot has actuation redundancy when it is driven by number of actuators greater than the degree of freedom. The actuation redundancy may increase the cost of the robot and complexity of control. However, the actuation redundancy is one of the most effective methods for avoiding the singularity during the mode change.

Figure 6 represents 3_PRR_ parallel robot, a planar two-dof parallel robot redundantly actuated three actuators. The Jacobian of the parallel robot is given as

$$\mathbf{J}_x \dot{\mathbf{x}} = \mathbf{J}_q \dot{\mathbf{q}} \tag{17}$$

$$\mathbf{x} = \begin{bmatrix} \dot{x} & \dot{y} \end{bmatrix}^T, \mathbf{q} = \begin{bmatrix} q_1 & q_2 & q_3 \end{bmatrix}^T$$

$$\mathbf{J}_x = \begin{bmatrix} \mathbf{w}_1^T \\ \mathbf{w}_2^T \\ \mathbf{w}_3^T \end{bmatrix}, \mathbf{J}_q = \begin{bmatrix} \mathbf{w}_1^T \mathbf{u}_1 & 0 & 0 \\ 0 & \mathbf{w}_2^T \mathbf{u}_2 & 0 \\ 0 & 0 & \mathbf{w}_2^T \mathbf{u}_2 \end{bmatrix}$$

where $\mathbf{J}_x$ is 3×2 matrix of its full rank that equals two. For convenience, singularity analysis is applied to the 3×2 transposed Jacobian matrix of $\mathbf{J}_x^T$. When at least one 2×2 minor of $\mathbf{J}_x^T$ is nonsingular, the rank of the $\mathbf{J}_x$ equals two; namely, the $\mathbf{J}_x$ has full rank. At this time, the robot still works as two-dof parallel robot. For example, when the first rod and the second rod are collinear as shown in **Figure 6** (iii), 2×2 minors of the $\mathbf{J}_x^T$ become

$$\begin{cases} \det([\mathbf{w}_1 \quad \mathbf{w}_2]) = 0 \\ \det([\mathbf{w}_1 \quad \mathbf{w}_3]) \neq 0 \\ \det([\mathbf{w}_2 \quad \mathbf{w}_3]) \neq 0 \end{cases} \tag{18}$$

As shown in Eq. (18), one minor is singular and the other two minors are nonsingular; namely, the $\mathbf{J}_x$ still has the full rank.

Now, the parallel robot loses the redundancy but keeps the nonsingularity. The parallel robot can pass the singular configuration of **Figure 6** (iii). In the same way, the parallel robot can pass the singular configuration of **Figure 6** (ii). Thus, the parallel robot achieves the assembly mode change from **Figure 6** (i) to (iv).
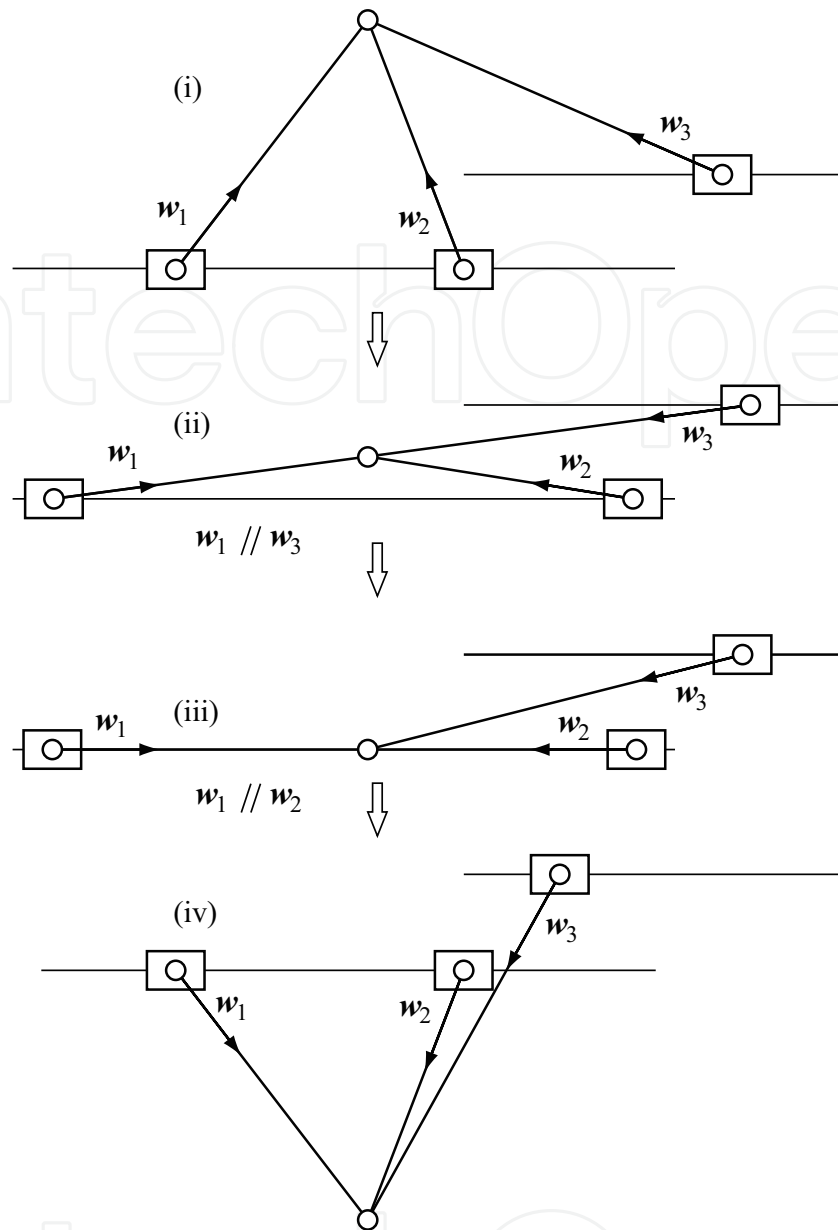
Figure 6. Assembly mode change of redundant 3*PRR* parallel robot.

2.4.2. Passing the first kind of singularity during the working mode change

The parallel robot encounters the first kind of singularity during the working mode change. In the velocity control of a robot, the velocity of the actuator is controlled to trace the desired velocity of the actuator $\dot{\mathbf{q}}_r$, which is given from the desired velocity of the end-point $\dot{\mathbf{x}}_r$ from Eq. (12) as

$$\dot{\mathbf{q}}_r = \left(J_q^{-1} J_x \right) \dot{\mathbf{x}}_r \tag{19}$$

However, $\mathbf{J}_q^{-1}$ cannot be calculated when $\mathbf{J}_q$ is singular at the first kind of singularity. In this case, the desired velocity of the actuator is directly given instead of being indirectly given from Eq. (12).

2.5. Researches on mode change of the parallel robot

Researches on expanding the workspace by the mode change of the parallel robot have been reported for nonredundant two-dof planar robot [4, 5], nonredundant three-dof spatial translational robot [6], redundantly driven three-dof translational and rotational planar robot [7], and redundantly driven three-dof spatial translational robot [8]. Redundant actuation is the actuation in one of the most effective methods for avoiding the singularity. However, the redundancy is not always the answer to avoiding the singularity. Additional ingenuities, for example, path planning for mode change, or asymmetrical design for the robot, are required.

3. Expanding the rotational workspace

3.1. Conventional methods

In this section, methods for expanding the rotational workspace of the parallel robot are introduced. **Figure 7(a)** represents the Stewart Platform [9], six-dof parallel robot with three-dof translations and three-dof rotations. The moving plate is driven by linear actuator embedded six limbs. Each limb is paired by a passive universal joint (U) with the base plate and paired by a passive spherical joint (S) with the moving plate. The Stewart Platform is categorized into 6$U\underline{P}S$ parallel mechanism. The Stewart Platform generates high power with a hydraulic linear actuator. Flight simulator and driving simulator for carrying heavy cockpit of aircraft are typical applications of the Stewart Platform. However, the robot has a drawback of small rotation around z axis because of the mechanical interference between the limbs. **Figure 7(b)** represents a six-dof cable-driven parallel robot [10]. This robot also has the same drawback of small rotation around z axis because of the cable interference. Small rotation of parallel robots puts restriction to their applications.
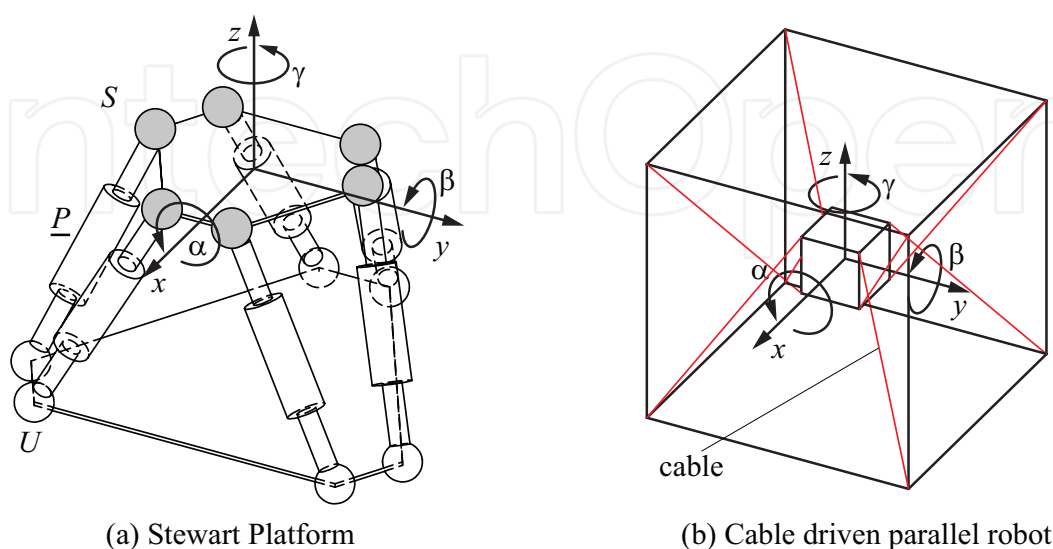

(a) Stewart Platform   (b) Cable driven parallel robot

Figure 7. Conventional six-dof parallel robot.

In order to cope with the problem, Clavel invented a novel parallel robot DELTA [11] as shown in **Figure 8**. The DELTA generates three-dof translation and one-dof rotation around the z-axis.

Three control arms are rotated by three motors located on the base plate. Each arm is connected to the moving part by a parallelogram rod with spherical joints. The gripper on the moving part is connected to the motor on the base plate with a telescopic arm via universal joints (**Figure 9**).

Researches on expanding the rotational workspace of the DELTA like parallel robot have been reported from research group at the Montpelier University. The basic idea is to convert the translational motion to the rotational motion by the mechanical gimmicks such as pulley, rack and pinion, and screw [12]. Crank embedded moving part has been proposed by McGill University for two-limb parallel robot [13] and by Fraunhofer IPA for cable-driven parallel robot [14].

3.2. Differential screw drive system

Recently, differential screw drive systems composed of two screw-nut pairs of different leads have been applied to robot systems [15, 16]. There are four driving methods of the differential drive systems;
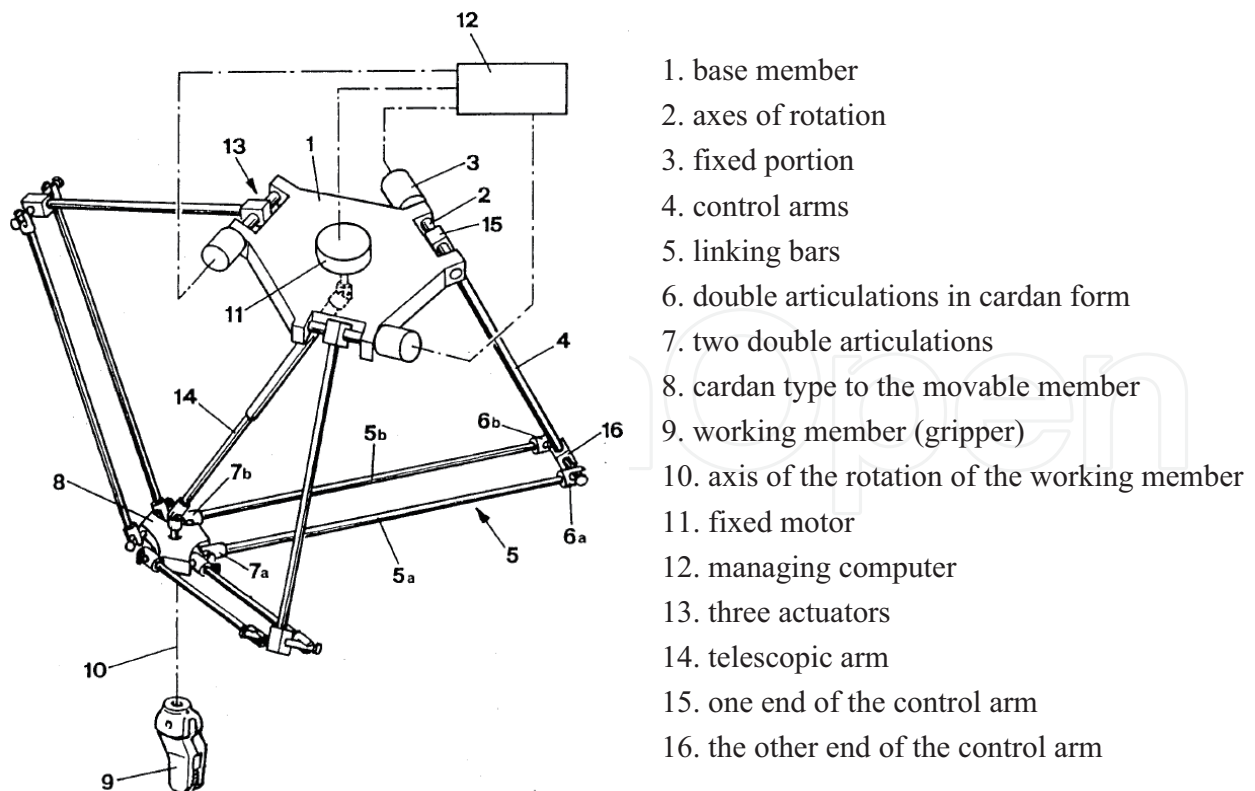

1. base member
2. axes of rotation
3. fixed portion
4. control arms
5. linking bars
6. double articulations in cardan form
7. two double articulations
8. cardan type to the movable member
9. working member (gripper)
10. axis of the rotation of the working member
11. fixed motor
12. managing computer
13. three actuators
14. telescopic arm
15. one end of the control arm
16. the other end of the control arm
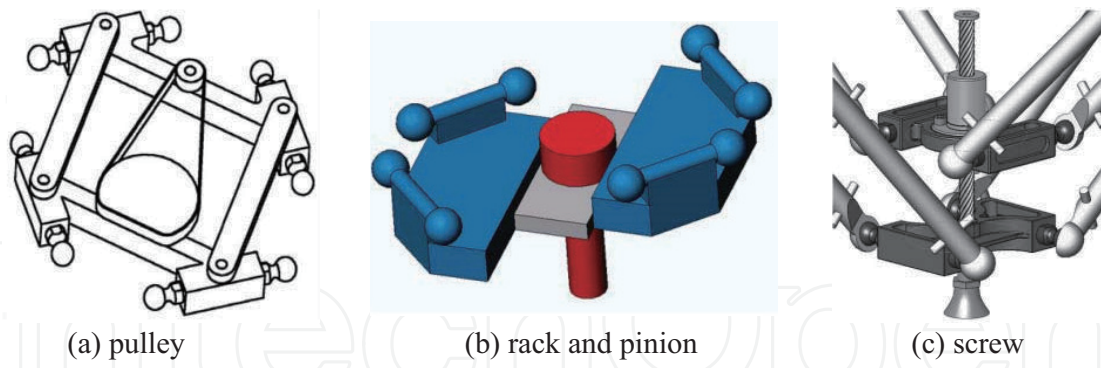
Figure 8. The DELTA robot [11].

Figure 9. Mechanical gimmicks enlarge the rotational workspace of parallel robot [12].

(a) Rotations of the two nuts are converted to the rotation and translation of the screw pair, which is coaxially arranged with one end interconnected with each other.

(b) Translations of the two nuts are converted to the rotation and translation of the screw pair, which is coaxially arranged with one end interconnected each other.

(c) Rotations of the two screws are converted to the rotation and translation of the nut pair, which is coaxially arranged with one end interconnected each other.

(d) Translations of the two screws are converted to the rotation and translation of the nut pair, which is coaxially arranged with one end interconnected each other.

In this section, kinematics of the differential drive system (b) as shown in **Figure 10** is discussed for enlargement of the rotational workspace of the parallel robot.

Let l_i $(i = 1, 2)$ be the lead of the ith screw nut. n_i $(i = 1, 2)$, z, and γ represent the position of the ith nut, position, and angle of the screw pair, respectively. Relation of these parameters is given as

$$n_i = z - \frac{l_i}{2\pi} \gamma \tag{20}$$

Equation (20) is given in the matrix form as

$$\begin{bmatrix} n_1 \\ n_2 \end{bmatrix} = \begin{bmatrix} 1 & -\dfrac{l_1}{2\pi} \\ 1 & -\dfrac{l_2}{2\pi} \end{bmatrix} \begin{bmatrix} z \\ \gamma \end{bmatrix} \tag{21}$$

Equation (21) gives the inverse kinematics of the differential drive system. The forward kinematics of the system is derived by inverting Eq. (21) as

$$\begin{bmatrix} z \\ \gamma \end{bmatrix} = \frac{1}{l_2 - l_1} \begin{bmatrix} l_2 & -l_1 \\ 2\pi & -2\pi \end{bmatrix} \begin{bmatrix} n_1 \\ n_2 \end{bmatrix} \tag{22}$$

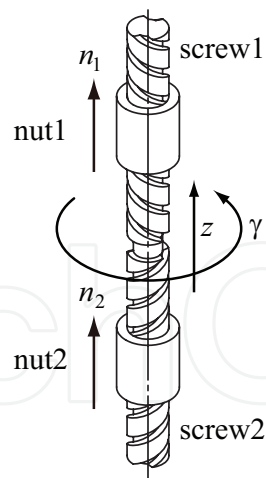If two leads of the screw-nut pair are identical as

$$l_1 = l_2 \tag{23}$$

Figure 10. Differential screw drive system (translations of the two nuts).

then the matrix in Eq. (22) becomes singular. It is necessary that the leads of the two screw nuts are different from the differential drive system.

Figure 11 represents a 4-dof parallel robot that the differential drive system (a) embedded in the moving part [15, 16]. H represents a passive helical joint composed of screw and nut pair. In **Figure 11**, two H pairs have the same lead, but the different helix hands (right and left). In **Figure 9 (c)**, one H pair and one R pair are embedded in the moving part. This is included in the differential drive system (a), one of the H pair has zero lead.
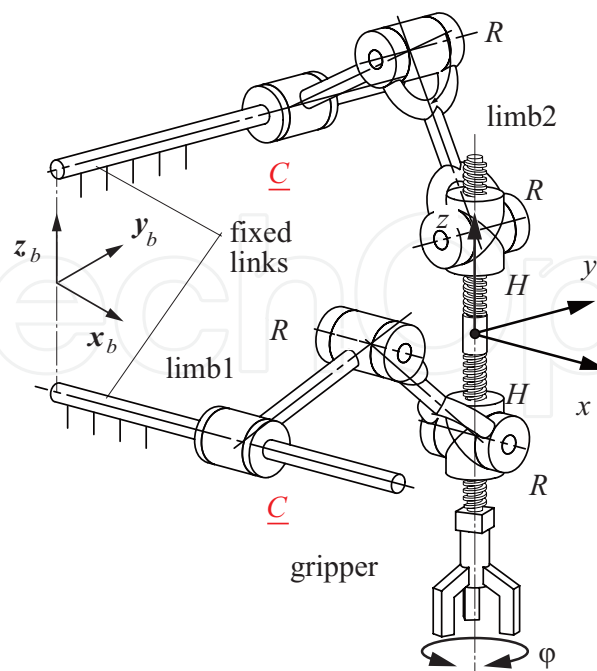

Figure 11. Parallel robot with the differential drive system embedded moving part [15].

4. Conclusion and future works

After commercialization of the DALTA robot, a lot of parallel robots can be found in machine factory and other industries. Recently, one can get the kit of a 3D printer machine by linear DELTA mechanism under 500 USD. It may be said that the first-generation parallel robot such as DELTA and Stewart Platform is getting to reach the mature stage. In this chapter, expanding the workspace of the parallel robot was introduced. The translational workspace was expanded by singularity-free mode change using the actuation redundancy. The differential drive mechanism converts the translational motion to the rotational motion, which expands the rotational workspace of the parallel robot. These parallel robots are expected as the next-generation robot.
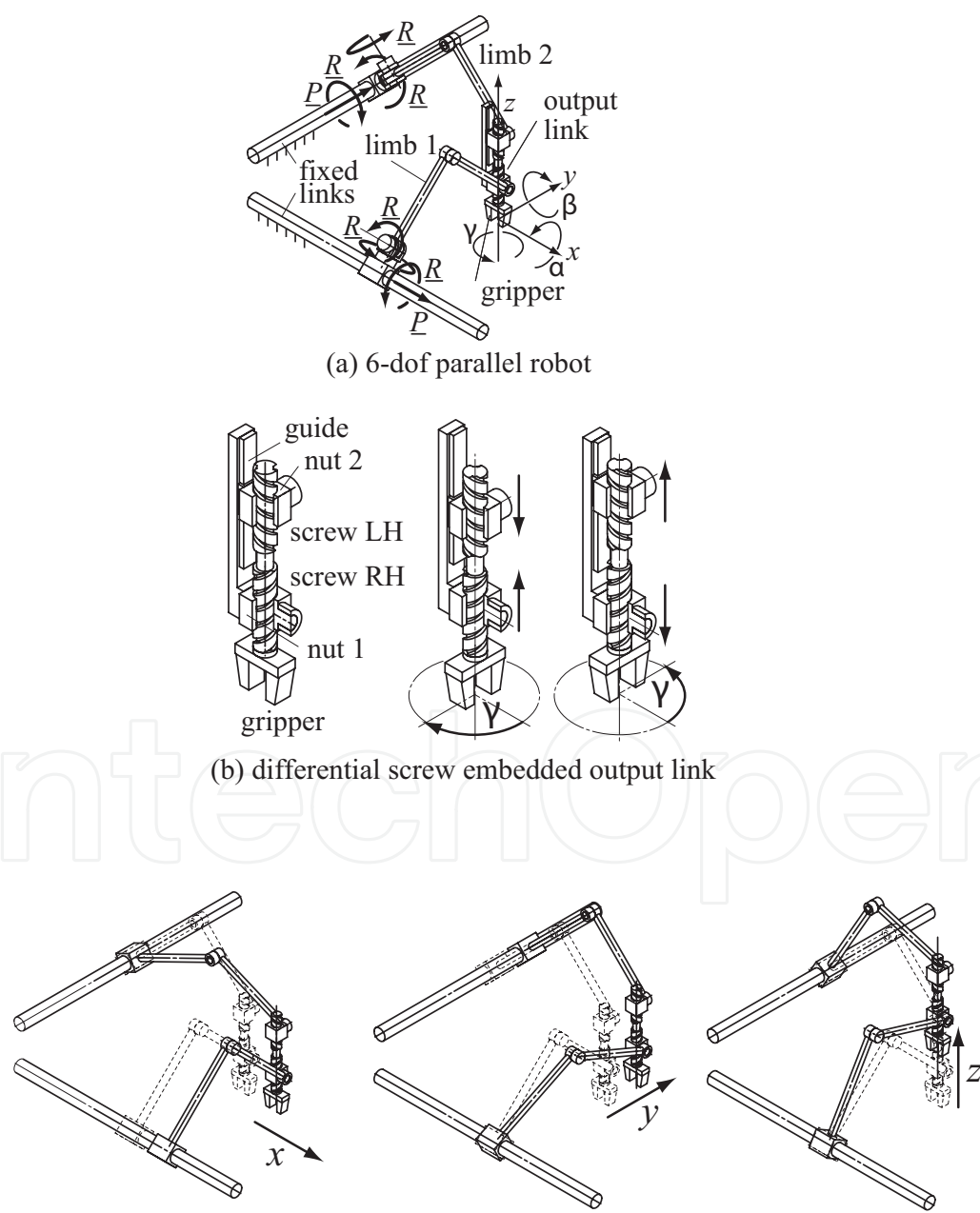
(a) 6-dof parallel robot

(b) differential screw embedded output link

Figure 12. Two-limb six-dof parallel robot with the differential drive embedded output link [18].

(a) translations along *x*, *y*, and *z* axis

(b) turnings around *x* and *y* axis

rotate by screws   rotate by limbs
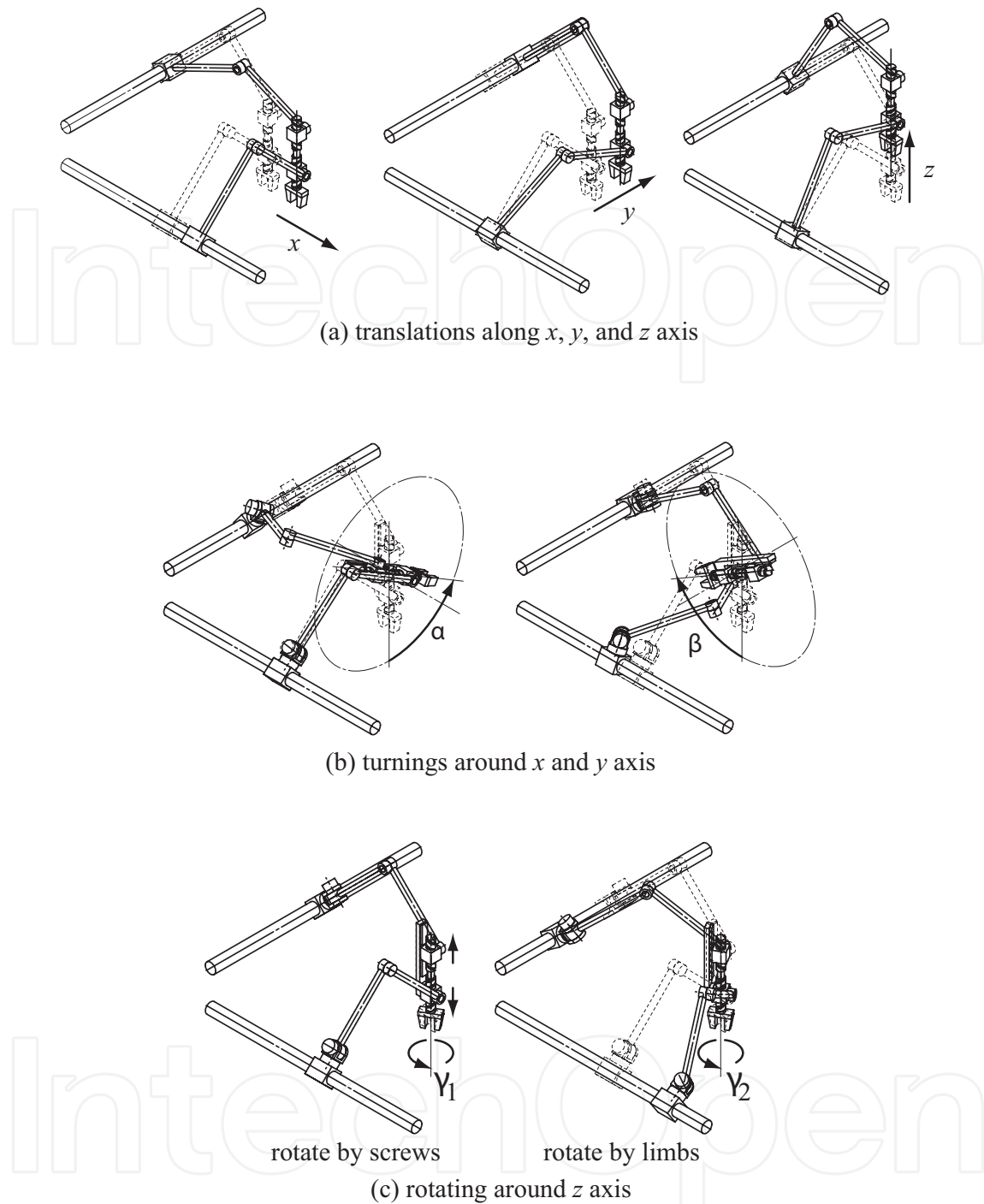(c) rotating around *z* axis

Figure 13. Motion of the two-limb six-dof parallel robot.

At the end of this chapter, an example of the next-generation parallel robot is introduced. **Figure 12(a)** represents a novel two-limb six-dof parallel robot [17]. As shown in **Figure 12(b)**, a differential screw mechanism is embedded in the output link for enlarging the rotational workspace of the gripper. This parallel robot extends its degree of freedom from four (three translations and one rotation as shown in **Figure 11**) to six (three translations and three rotations) as shown in **Figure 13**. We are working on the kinematic analysis and detailed mechanical design of the parallel robot [18].

Acknowledgements

Author details

Takashi Harada

Address all correspondence to: harada@mech.kindai.ac.jp

Department of Mechanical Engineering, Faculty of Science and Engineering,
Kindai University, Higashiosaka, Osaka, Japan

References

[1] Merlet JP. Parallel Robots. 2nd ed. Netherlands: Springer; 2006. 402 p. DOI: 10.1007/1-4020-4133-0

[2] Gosselin C, Angeles J. Singularity analysis of closed-loop kinematic chains. IEEE Transactions on Robotics and Automation. 1990;**6**(3):281-290. DOI: 10.1109/70.56660

[3] Tsai LW. Robot Analysis. 1st ed. New York: Wiley-Interscience; 1998. 520 p. ISSN: 978-0471325932

[4] Hesselbach J, Woffmeister H, Loohß T, Krefft M, Armbrecht C. Parallel kinematic concept for stationary high performance cutting in wood machining. Production Engineering. 2007;**1**(2):205-212. DOI: 10.1007/s11740-007-0033-9

[5] Campos L, Bourbonnais F, Bonev I and Bigras P. Development of a five-bar parallel robot with large workspace. In: Proceedings of the ASME 2010 International Design Engineering Technical Conferences & Computers and Information in Engineering Conference; 15-18 August 2010; Montreal. 2010. pp. 917-922. DOI: 10.1115/DETC2010-28962

[6] Budde C, Last P and Hesselbach J. Development of a triglide-robot with enlarged workspace. In: Proceedings of IEEE International Conference on Robotics and Automation; 10-14 April 2007; Roma. 2007. pp. 543-548. DOI: 10.1109/ROBOT.2007.363043

[7] Harada T. Mode changes of a planar 3 DOF redundantly actuated parallel robot. International Journal of Materials, Mechanics and Manufacturing. 2016;**4**(2):123-126. DOI: 10.7763/IJMMM.2016.V4.238

[8] Harada T. Mode changes of redundantly actuated asymmetric parallel mechanism. Journal of Mechanical Engineering Science. 2015;**230**(3):454-462. DOI: 10.1177/0954406215588479

[9] Steward D. A platform with six degrees of freedom. Proceedings of the Institution of Mechanical Engineers. 1965;**180**(1):371-386. DOI: 10.1243/PIME_PROC_1965_180_029_02

[10] Bruckmann T, Pott A, editors. Cable-Driven Parallel Robots. 1st ed. New York: Springer; 2013. 454 p. DOI: 10.1007/978-3-642-31988-4

[11] Clavel R. Device for the Movement and Positioning of an Element in Space. US Patent No. 4,976,582. 1989

[12] Company O, Pierrot F, Krut S, Nabat V. Simplified dynamic modelling and improvement of a four-degree-of-freedom pick-and-place manipulator with articulated moving platform. Journal of Systems and Control Engineering. 2009;**223**(1):13-29. DOI: 10.1243/09596518JSCE616

[13] Gauthier J, Angeles J, Nokleby SB, Morozov A. The kinetostatic conditioning of two-limb schonflies motion generators. Transactions of the ASME Journal of Mechanisms and Robotics. 2008;**1**(1):011010. DOI: 10.1115/1.2960544

[14] Miermeister P, Pott A. Design of cable-driven parallel robots with multiple platforms and endless rotating axes. In: Kecskeméthy A, Flores FG, editors. Interdisciplinary Applications of Kinematics. 1st ed. Lima: Springer; 2013. p. 21-29. DOI: 10.1007/978-3-319-10723-3_3

[15] Harada T, Angeles J. Kinematics and singularity analysis of a CRRHHRRC Schönflies motion generator. Transactions of the Canadian Society for Mechanical Engineering. 2014;**38**(2):173-183. ISSN: 0315-8977

[16] Harada T, Friedlaender T and Angeles J. The development of an innovative two-DOF cylindrical drive: Design, Analysis and preliminary tests. In: Proceedings of IEEE International Conference on Robotics and Automation; 31 May-7 June 2014; Hong Kong. 2014. pp. 6338-6344. DOI: 10.1109/ICRA.2014.6907794

[17] Harada T and Makino T. Design of a novel 6 DOF parallel robot for haptic device. In: 12th International Conference on Ubiquitous Healthcare; October 30–November 2; Osaka, Japan. 2015

[18] Harada T and Angeles J. From the McGill Pepper-Mill Carrier to the Kindai Atarigi Carrier. In: Proceedings of the 2017 IEEE International Conference on Robotics and Biomimetics; December 5-8; Macau SAR, China. 2017. Printing